

1 **Effects of a nuclear power plant warmwater outflow on environmental conditions and**
2 **fish assemblages in a very large river (the Danube, Hungary)**

3

4

5 V. Füstös^{1,2}, P. Sály^{3,4}, Z. Szalóky^{3,4}, B. Tóth⁵, Z. Vitál⁶, A. Specziár^{2,7}, G. Fleit^{1,8,9}, S. Baranya^{1,9}, J.
6 Józsa^{1,8,9}, T. Erős^{2,7*}

7

8 ¹ *Department of Hydraulic and Water Resources Engineering, Faculty of Civil Engineering, Budapest*
9 *University of Technology and Economics, Műegyetem rkp. 3., H-1111 Budapest, Hungary*

10 ² *Balaton Limnological Research Institute, ELKH, Klebelsberg Kuno u. 3., H-8237 Tihany, Hungary*

11 ³ *Institute of Aquatic Ecology, Centre for Ecological Research, Karolina út 29., H-1113 Budapest,*
12 *Hungary*

13 ⁴ *National Laboratory for Water Science and Water Security, Institute of Aquatic Ecology, Centre for*
14 *Ecological Research, Karolina út 29., H-1113 Budapest, Hungary*

15 ⁵ *Danube-Ipoly National Park Directorate, Költő u. 21., H-1121 Budapest, Hungary*

16 ⁶ *Research Institute for Fisheries and Aquaculture, National Agricultural Research and Innovation*
17 *Centre, Anna-liget utca 35., H-5540 Szarvas, Hungary*

18 ⁷ *National Laboratory for Water Science and Water Security, Balaton Limnological Research Institute,*
19 *ELKH, Klebelsberg Kuno u. 3., H-8237 Tihany, Hungary*

20 ⁸ *MTA-BME Water Management Research Group, Budapest, Hungary*

21 ⁹ *National Laboratory for Water Science and Water Security, Department of Hydraulic and Water*
22 *Resources Engineering, Faculty of Civil Engineering, Budapest University of Technology and*
23 *Economics, Műegyetem rkp. 3., H-1111 Budapest, Hungary*

24

25 *Corresponding author:

26 Tibor ERŐS

27 Balaton Limnological Research Institute, ELKH

28 Klebelsberg K. u. 3., H-8237 Tihany, Hungary

29 E-mail address: eros.tibor@blki.hu

30

31

32 Abstract

33 Direct or indirect effects of nuclear power plants' (NPPs) warmwater effluents on the structure
34 of biotic assemblages are poorly known in very large rivers. We examined changes in physical
35 habitat structure, temperature condition and their possible effects on the structure of Danubian
36 fish assemblages due to the outflow of the Paks NPP's warmwater channel, in Hungary.
37 Seasonal surveys conducted both upstream and downstream from the outfall showed that its
38 hydromorphological effects were generally local and comparable to natural or other
39 anthropogenic hydromorphological changes. The effect of the returned cooling water was more
40 apparent in the seasonally recorded surface water temperatures and depended highly on the
41 spatial positioning of the sampling sites. However, environmental and spatial variables
42 accounted only for a low amount of variance in case of both shoreline and offshore fish
43 assemblage data. Overall, we found that the outflow exerted only a local scale effect on the
44 structure of Danubian fish assemblages. Rather, fish assemblages varied largely both inshore
45 and offshore, which dynamics overruled any effects of the artificially elevated temperature. Our
46 study highlights the importance of the assessment of hydrogeomorphological variability of
47 rivers and their influence on fish assemblage variability when examining spatial effects of
48 thermal pollution.

49

50

51

52 Key words: thermal pollution, habitat use, fish, geomorphology, substrate, Danube River

53

54 Running head: effects of a warmwater outflow in a very large river

55

56 **1. Introduction**

57 Anthropogenic stressors influence aquatic ecosystems in a variety of ways. Of these, physical
58 habitat alterations and the human assisted spread of invasive species are among the top cited
59 factors, which threaten the diversity and integrity of aquatic ecosystems (Dudgeon et al., 2006;
60 Reid et al., 2019). Although less studied, but the destruction of the habitat is often accompanied
61 by thermal and chemical pollution, which may magnify the effect of hydrological and/or
62 geomorphological modifications (Teixeira et al., 2009; Erős et al., 2015).

63 Nuclear energy plays an important role in the electricity production of the world, comprising
64 cca. 14% of the electric energy needs (Karakosta et al., 2013). Beside clearly renewable energy
65 sources (e.g., solar radiation, wind) nuclear power plants (NPPs) contribute significantly to
66 mitigating greenhouse gas emissions (Adamantiades and Kessides, 2009). On the other hand,
67 the public acceptance of nuclear energy is low, which is mainly due to the problems of handling
68 radioactive waste and safety reasons. Although less known by the public, the operation of NPPs
69 needs a significant amount of cold water to control condenser process temperature. The wasted
70 (thus heated) cooling water is then emptied back to the recipient aquatic environment, which
71 may present a thermal pollution for the biota (Raptis et al., 2016).

72 Studies on the effect of thermal pollution on ecological assemblages have yielded controversial
73 results. For example, detailed studies highlighted the decline of brown macroalgae assemblages
74 to thermal stress from the effluent discharge of NPPs in coastal marine environments (Schiel et
75 al., 2004; Széchy et al., 2017). On the other hand, no significant effect on coral reef fish
76 assemblages was observed around an NPP in southern Taiwan (Jan et al., 2001). Another study
77 in a coastal environment in Southeastern Brasil showed that fish species richness and diversity
78 (Shannon–Wiener index) was negatively influenced by the thermal pollution from an NPP
79 (Teixeira et al., 2009, 2012). However, the effect depended also on the diversity of habitat
80 structure. In complex habitats, where physical habitat diversity was high, fish assemblages were
81 unaffected by thermal pollution (Teixeira et al., 2012). Although studies from freshwater
82 environments are limited, these studies show the controversial effects of thermal pollution from
83 NPPs on ecological assemblages (see e.g., Descy and Mouvet, 1984; Daufresne et al., 2003).
84 Overall, further studies are needed from a variety of aquatic environments for a detailed
85 understanding of the effect of NPP effluents on the community organization of aquatic
86 organisms.

87 Our study target, the Paks NPP is situated in Hungary directly at the right bank of the very large
88 Danube River. The power plant is operated by four pressurized-water reactor blocks. The
89 cooling water of the NPP is obtained directly from the Danube, and the used (warmed) water is
90 returned to the Danube through the warmwater channel. The channel has an approximate
91 discharge of $100 \text{ m}^3 \text{ s}^{-1}$ in the majority of the year, when all of the four blocks of the NPP are
92 operating (Janovics et al., 2014). Such a discharge is equal to the discharge of a medium sized
93 river, and consequently may substantially influence the environmental conditions of the
94 mainstem Danube (mean discharge at the study reach is $2300 \text{ m}^3 \text{ s}^{-1}$, while the lowest navigable
95 discharge, which may last for weeks, is $1240 \text{ m}^3 \text{ s}^{-1}$). The confluence zones of rivers are
96 generally characterized by complex hydro- and morphodynamic features (e.g., Bradbrook et
97 al., 2000; Rhoads and Sukhodolov, 2001; Baranya et al., 2015). These locally varying

98 hydrological and morphological conditions can affect the organization of ecological
99 assemblages (Rice et al., 2006). The focus of recent studies (e.g. Czeglédi et al., 2015; Erős and
100 Lowe, 2019) is a thorough understanding of the significance of tributary effects on the
101 mainstem river in a variety of hydrological, geomorphological and topographic conditions (e.g.,
102 discharge, substratum composition, relative size of the tributary and the mainstem river,
103 network position in the catchment).

104 In this study we assessed the effect of the artificial tributary of the NPP on the abiotic and biotic
105 conditions of the Danube River. We addressed the following questions: i) How does the warm
106 water effluent of the Paks NPP influence the thermal and hydromorphological characteristics
107 of the Danube, ii) Do changes in abiotic conditions influence the structure of Danubian fish
108 assemblages?

109

110 **2. Material and methods**

111 *2.1. Study area*

112 The Danube has a drainage area of approximately 800,000 km². River regulation, namely the
113 construction of hydroelectric schemes, especially in the Upper Danube (i.e., in Germany and
114 Austria), and channelization have profoundly modified the physical structure of the Danube
115 throughout its course. The Hungarian reach (Fig. 1), referred to as the 'Middle Danube', runs
116 for 417 km and has a mean annual discharge of ~2000 m³ s⁻¹. The main channel has a
117 substratum dominated by gravel and sand, a mean depth of 4 m and a mean flow velocity of
118 1.3 m s⁻¹. The banks are relatively natural (except the section lying within Budapest, the capital
119 of Hungary), interrupted with embanked rip-rap shorelines of ~ 100-1000 m long sections. The
120 studied segment (i.e., between 1535-1520 rkm) of the Paks NPP is a typical representative of
121 the Hungarian reach of the river. Here, the substrate is dominated by sand and fine gravel. The
122 river bank is partly modified by rip-rap embankments and groins to enhance navigation.

123 *2.2. Data collection*

124 Altogether three sampling campaigns were conducted in the studied 15 km long reach in spring
125 2020 (19-21 May) in summer 2020 (21-23 July) and autumn 2020 (15-17 September). Within
126 the study reach we selected eight 500 m long subreaches (Fig. 1) to explore the effect of the
127 NPP on the abiotic characteristics and fish assemblages of the Danube. Of these, three
128 subreaches situated upstream of the warm effluent, and consequently were not influenced by
129 the NPP. On the other hand, five subreaches were selected downstream of the outfall. These
130 were thus supposed to be influenced by the thermal water to a varying degree.

131 *Hydromorphological data and temperature measurements*

132 Water depth and flow velocity were mapped within each subreach along equidistant transects,
133 50 m apart, by a Teledyne (USA) RDI Rio Grande Workhorse 1200 KHz Acoustic Doppler
134 Current Profiler (ADCP) mounted on a 6 m long measurement vessel. Instantaneous vertical
135 velocity profiles and flow depth values were recorded by the ADCP in every 1.3 seconds. A
136 Stonex (Italy) S9 Real Time Kinematic (RTK) GPS connected to the ADCP recorded the vessel

137 position simultaneously. For the follow-up analysis, depth-averaged flow velocity values were
138 derived from the vertical profiles. The density of the surveyed transects, 11 within the 500 m
139 long subreach, allowed linear interpolation of both the velocity and depth values. Accordingly,
140 two-dimensional maps of water depth and depth-averaged flow velocity could be derived for
141 each subreach.

142 The bed material was sampled during the first (spring) campaign at five points along the central
143 cross-section in each subreach, collecting altogether 40 samples. In the four-month time period
144 covering our seasonal measurements, the discharge of the Danube remained under $4500 \text{ m}^3 \text{ s}^{-1}$.
145 Due to the lack of a higher flood during the study period, it could be assumed that the bed
146 material composition did not change significantly after the spring sampling, thus no additional
147 samplings were done. A metal bucket sampler was trawled on the riverbed for a short time and
148 a bulk sample was retrieved. The exact location and the flow conditions were recorded
149 simultaneously by the GPS and ADCP, respectively. The bed material samples were dried and
150 sieved with a Retsch (Germany) AS 450 Basic vibratory sieve shaker to determine grain size
151 distribution.

152 Water temperature was recorded in two aspects: along cross-sections near the surface by the
153 ADCP and along depth in the verticals of the bed material sampling locations. The vertical
154 samplings were performed by a Teledyne (USA) Digibar S sound velocity profiler. The exact
155 location and the flow conditions were recorded simultaneously by the GPS and ADCP,
156 respectively. The cross-sectional temperature data was also dense enough for linear
157 interpolation in the data processing stage, similarly to water depth and depth-averaged flow
158 velocities. Temperatures along water depth were used to determine spatial variability,
159 particularly near the NPP effluent.

160 *Fish collections*

161 Fish were collected using shoreline electric fishing and offshore benthic trawling. For the
162 sampling of shoreline fish assemblages, 17 (spring 2020) and 18 (summer and autumn 2020)
163 500 m long rip-rap or natural shoreline stretches were selected (Fig. 1), along the same
164 subreaches where the hydromorphology was revealed. Rip-rap stretches can be characterized
165 as rock and boulder covered artificial banks, while natural stretches lack any apparent shoreline
166 engineering measures and have a general substratum type of sand and fine gravel (Erős et al.,
167 2008). The ratio of natural and rip-rap stretches represented the distribution of these two main
168 shoreline mesohabitat types. The 500 m long units were electrofished from a boat, using a Hans
169 Grassl GmbH (Germany) EL64 IIGI, DC, 7.5 KW device. Fish were caught with a hand held
170 anode (2.5 m long pole with a ring anode of 40 cm diameter and a net mesh size of 6 mm) while
171 slowly moving downstream with the boat as per Wolter and Freyhof (2004). The cathode, a 3 m
172 long copper cable, was floated at the rear of the boat. We used nighttime sampling because
173 former surveys of the Danube (Erős et al., 2008) and other surveys (Wolter and Freyhof, 2004)
174 justified that it is more efficient than daytime sampling of shoreline fish assemblages. At the
175 end of each 500-m unit, captured fish were identified, counted and returned into the water.

176 Offshore distribution of fish was examined using an electrified benthic framed trawl (Szalóky
177 et al., 2014). In each subreach (Fig. 1), across the width of the main channel, we distributed 5

178 trawl paths, 500 m long each, excluding the littoral, less than 2 m deep shoreline zone. These
179 paths were approximately equispaced and centered over the approximate place of the main
180 channel centerline (Gutreuter et al., 2009), at the place where abiotic (i.e., bed material) samples
181 were also collected. The trawl consisted of a stainless-steel frame (2 m wide \times 1 m high) of
182 which a drift net was attached (mesh size 5 and 8 mm for the inner and outer mesh bag,
183 respectively) (for details see Szalóky et al., 2014). The frame was electrified with a Hans Grassl
184 GmbH (Germany) EL65 IIGI electrofishing device operated with a VANGUARD (USA) HP21
185 14.9 KW generator. A 6 m long copper cathode cable was connected freely and pulled approx.
186 2 m before the electrified frame. The fishing team consisted of two people handling the framed
187 net, one handling the electrofishing device and one operating the boat. Trawling was conducted
188 during daytime with a 6.3 m long boat powered by a 50-horsepower outboard Mercury (USA)
189 four stroke engine. Before starting trawling, the operators lowered the frame to the bottom while
190 the boat was slowly moving downstream with the flow. Trawling route was started to be
191 measured by a GARMIN (USA) GPSMAP 60CSx only after the net reached the bottom, which
192 could be easily felt while holding the central rope, and right after electroshocking started. The
193 direct current (approx. 350 V, 33 A) was applied for 5-8 s with 3-5 s breaks between the
194 operations to minimize fright bias and injury of fish. The applied trawling speed was slightly
195 higher than the current velocity of the river (approx. 1.3 m s⁻¹). The collected fish were
196 identified, measured to the nearest mm standard lengths and then released back to the river.

197 *2.3. Statistical analysis*

198 General linear models with normal error distribution and identity link function were used to
199 examine how 1) the bank side (i.e., right vs. left side of the river; the NPP effluent is on the
200 right bank of the Danube), 2) the location of the sampling site (upstream vs. downstream from
201 the effluent) and 3) the season (spring, summer or autumn) were related with temperature values
202 of inshore samples. Similarly, linear models were used to explore how 1) the position of
203 offshore samples (here position of the sample along each subreach across the width of the main
204 channel), 2) the location of the sampling site (upstream vs. downstream from the effluent) and
205 3) the season (spring, summer or autumn) were related with temperature values of offshore
206 samples. The models were built considering all interaction effects of the three factors. Then,
207 model selections were conducted to identify the minimal adequate models, which hold only
208 significant ($P \leq 0.05$) terms (Crawley 2015). This explorative analysis revealed strong
209 relationships between water temperature and the three tested factors in case of both the inshore
210 and offshore samples (see the Results section). This finding suggested that the effect of
211 temperature could not be disentangled from the effect of the spatial positioning of the sampling
212 sites and the season. Therefore, the factors of spatial positioning (i.e., bank side, location
213 regarding the power plant outflow, and position along the cross-section) were used as effectors
214 to test the influence of the power plant on the habitat and fish assemblage in the further data
215 analyses.

216 Redundancy analyses were used to test how position and location of the sampling sites, season
217 and the examined environmental variables, such as depth, velocity and substrate composition
218 influenced the species richness and assemblage structure (i.e., relative abundance) of the fish
219 communities for both the shoreline electrofishing and the bottom trawling data. The examined

220 environmental variables (specifically mean depth, mean velocity, %silt, %sand, %gravel,
221 %pebble, %cobble) were considered as conditional variables in the models to dissect the
222 influence of spatial positioning and related temperature effects on the structure of fish
223 assemblages from those caused by hydrogeomorphological variability. Species richness data
224 (i.e., number of species captured in the 500 m long sampling units) were $\ln(x+1)$, while
225 abundance-based fish assemblage data (i.e., number of individuals of each species captured in
226 the 500 m long sampling units) were Hellinger transformed before the analyses. Species
227 occurring in less than three sampling units had been removed and the conditional variables had
228 been normalized to zero mean and unit variance in the abundance-based analyses.

229

230 **3. Results**

231 *3.1. Environmental effects of the warmwater outflow*

232 The flow discharges in the Danube were 1700, 2700 and 1800 m³ s⁻¹ during the spring, summer
233 and autumn campaigns, respectively. Accordingly, larger water depth values were recorded in
234 summer (Fig. 2). Mean water depth varied between 4-6 m between the seasonal surveys.
235 Morphological features typical to a meandering reach can be observed on the depth maps.
236 Cross-section shapes at river bends (subreach No. 3, 5, 6) show asymmetric character, whereas
237 inflexion reaches (e.g., subreach No. 2, 7, 8) are more complex, indicating shallow regions in
238 the middle of the channel.

239 Depth-averaged flow velocities showed a strongly varying pattern among the subreaches
240 (Fig. 3). Maximum flow velocities varied between 1.4 and 1.6 m s⁻¹ between seasons. The
241 warm effluent affected the flow conditions to some extent. Specifically, the confluence of the
242 outflow narrowed the streamline in the subsequent subreach No. 4, compared to other
243 subreaches. Moreover, the groin at the right bank (Fig. 3) further narrowed the channel,
244 resulting in increased flow velocity in the main stream and close to zero flow velocities in the
245 recirculation zone downstream of the groin. Among the studied subreaches, this was the most
246 complex in terms of the flow field.

247 The bed material composition was dominated by sand, gravel and pebble in each subreach
248 (Fig. 4). The proportion of silt (<0.25 mm) and cobble (>64 mm) were uniformly very small
249 and zero, respectively. The spatial variability of the bed composition was low, the sand content,
250 however, was somewhat higher at the first and last subreaches. Overall, the effluent did not
251 seem to affect the subreach grain size composition of the bed material.

252 The effect of the returned cooling water was more apparent in the seasonally recorded surface
253 water temperatures than on hydromorphological features of the river (Fig. 5). The operational
254 temperature of the cooling water is constantly 10°C higher than the ambient temperature of the
255 river. The differences we measured, however, remained under 4°C, due to the mixing induced
256 cooling between the outfall and the subreaches. The highest differences (3-4°C) were observed
257 in subreach No. 4, which was nearest and thus most affected, at 200 m distance from the
258 effluent. The temperature gradient continuously decreased downstream, with a weakening rate
259 however, and remained at least 1-2°C within the investigated reach. Although the warmwater

260 plume somewhat widened, in the last two subreaches only the nearbank regions seemed to be
261 affected. Within the studied ~8 km reach downstream of the warmwater outfall, no complete
262 mixing took place. It is important to note that the warmer water affected the side arms along
263 the right bank, too.

264 General linear models showed significant relationships between water temperature and the
265 spatial factors and season. Specifically, shoreline temperature (Table 1) depended on the three-
266 way interaction of the bank side, location, and season ($\text{adj}R^2 = 0.99$, $F_{11,41}=643.9$, $p<0.001$),
267 indicating that the variability of temperature values in a given season could be explained by
268 both the bank side and location (upstream vs. downstream from the outflow) of the sampling
269 sites. In case of the offshore samples (Table 2), temperature values depended on the two-way
270 interaction of the position along the cross-section and location, and also on the two-way
271 interaction of the location and the season ($\text{adj}R^2 = 0.96$, $F_{29,90}=111.7$, $p<0.001$). These results
272 show that water temperature varied according to the location but its magnitude was highly
273 controlled by the position along the cross-section, and that the variability caused by the location
274 was also driven by the seasons (Fig. 5).

275 3.2. Fish assemblages

276 A total of 16,398 fish specimens were collected during the seasonal surveys and identified to
277 36 species (Table 3). Shoreline electrofishing yielded a larger number of species compared with
278 offshore trawling, independently of the season. The bleak, *Alburnus alburnus* (49.53%); round
279 goby, *Neogobius melanostomus* (11.42%); white-finned gudgeon, *Romanogobio vladykovi*
280 (9.61%) and the white bream, *Blicca bjoerkna* (8.71%) were the most dominant species in the
281 shoreline samples, but beside these, many species proved to be relatively abundant in the
282 shoreline samples. On the contrary, only a few species were dominant in the offshore samples
283 including the white-finned gudgeon, *Romanogobio vladykovi* (41.47%); the round goby,
284 *Neogobius melanostomus* (29.64%) and the Danube streber, *Zingel streber* (13.17%).

285 Albeit significant, the spatial and environmental variables accounted only for a low amount of
286 variance of species richness in case of the shoreline electrofishing samples ($\text{adj} R^2 = 0.1854$).
287 The covariant environmental variables (i.e., velocity, depth and substrate composition)
288 explained a much higher proportion of the variance (47.5%), than the spatial variables (24.9%).
289 Overall, the three-way interaction of season, location and position variables was responsible for
290 the variance in species richness (Table 4). The variance in species richness explained by
291 environmental and spatial variables was also low for the offshore trawling samples
292 ($\text{adj} R^2 = 0.2667$). However, here the covariant environmental variables explained a lower
293 proportion of the variance (15.3%), than the spatial variables (40.5%). Interestingly, a strong
294 effect of season was observed on species richness (Table 5), but it is important to note, that the
295 three-way interactions of season, location and position was only marginally insignificant
296 ($p=0.063$).

297 Similarly to species richness, only a low amount of variance of assemblage structure (Hellinger
298 transformed abundance data) could be explained by environmental and spatial variables
299 ($\text{adj} R^2 = 0.1730$) for the shoreline electrofishing samples. The covariant environmental
300 variables (i.e., velocity, depth and substrate composition) explained a higher proportion of the

301 variance (45.2%), than the spatial variables (24.7%). Again, a three-way interaction of season,
302 location and position was found to be responsible for the variance in the assemblage structure
303 (Table 6). Environmental and spatial variables accounted only for a very low proportion of
304 variance in the offshore structure of fish assemblages ($\text{adj } R^2 = 0.0865$). The covariant
305 environmental variables explained a lower proportion of the variance (17.2%) than the spatial
306 variables (27.5%). Beside the effect of the covariant environmental variables, seasonal effects
307 and inner position within a subreach was the most important determinant of the offshore fish
308 assemblage structure, while the impact of location (i.e., upstream or downstream from the
309 outflow) proved to be insignificant (Table 7).

310

311 **4. Discussion and conclusions**

312 Several studies have shown that tributary confluences influence hydromorphological conditions
313 of recipient rivers, the extent of which depends on many factors (e.g., Bradbrook et al., 2000;
314 Rhoads and Sukhodolov, 2001; Benda et al., 2004; Rice et al., 2006; Jones and Schmidt, 2017).
315 For example, the flow pattern at confluences is mainly influenced by the horizontal alignment
316 of the merging channels, the local morphological alterations and the unstable shear layer
317 between the two flows at different speed (Bradbrook et al., 2000). The ratio of the flow
318 discharges also plays an important role (e.g., Baranya and Józsa, 2007). The mixing and
319 transport of sediments and pollutants is also strongly determined by the local
320 hydromorphological features at confluences (Boyer et al., 2006; Szupiany et al., 2009; Baranya
321 et al., 2015). In our study system the observed local hydromorphological effects of the NPP
322 outflow were comparable to natural or other human induced hydromorphological changes. For
323 example, the natural bending of the river generating secondary flow components has a
324 deterministic role in the spatial variation of the flow velocity field, showing, in fact, a more
325 important factor than the returned cooling water of the NPP. Similarly, both flow depth and
326 velocity maps show that the mesoscale effects of riverbed meandering, the presence of groins,
327 side arms, point and side bars were more important determinants of hydromorphological
328 changes than that caused by the effluent (Fig. 2, 3). In addition, the warm water does not
329 transport sediment, which could alter the substrate composition of the mainstem. Therefore,
330 although deposition bars of debris and shells were observed in the vicinity of the confluence,
331 tributary effects of the NPP outflow were only very local and confined to a not more than 500 m
332 long segment downstream the outfall.

333 Temperature effects, on the contrary, were larger, and clearly distinguishable from the
334 background natural values. Although the largest difference in temperature was observed in the
335 subreach right below the effluent (subreach No. 4), differences in temperature were clear
336 between the left and right banks of course exclusively downstream of the effluent in each
337 subreach. Although it is clear that temperature effects of the NPP outflow may depend
338 substantially on discharge and temperature differences between the warmwater channel and the
339 recipient river, most studies have showed substantial decrease of temperature along a spatial
340 gradient from the effluent in both coastal areas and rivers (Daufresne et al., 2003; Teixeira et
341 al., 2012) – similarly to our findings.

342 Environmental and spatial variables accounted only for a low amount of variance in case of
343 both shoreline and offshore fish assemblage data. Such a low amount of variability is not
344 surprising, especially offshore, where the relatively short within-segment environmental
345 gradients (deep water, relatively uniform velocity and substrate conditions) make assemblage
346 structure hardly predictable (Wolter and Freyhof, 2004; Szalóky et al., 2021). Similarly to other
347 studies, seasonal changes accounted for a relatively large proportion of variation in the data.
348 These changes can be due to seasonal variations in flow regime and temperature (and related
349 capture efficiency effects), partial migrations of fish between different segments of the river
350 and their side arms and population dynamics of young of the year fish (Matthews, 1998; Wolter
351 and Bischoff, 2001).

352 Environmental variables were the major determinant of shoreline fish assemblage structure
353 (both richness and relative abundance). This indicates that variations in substrate composition,
354 depth, and velocity were more important variables in structuring fish assemblages than spatial
355 and associated temperature related variability inshore. Our former study in the Hungarian reach
356 of the Danube indicated that species richness of the two major habitat types (i.e., natural sand
357 and gravel dominated shorelines vs. stone and boulder covered rip-raps) did not significantly
358 differ at night, but the composition and relative abundance of the species may differ largely
359 (Erős et al., 2008). Unfortunately, the distribution of natural and rip-rap covered stretches were
360 not ideal in the study system to clearly test and dissect the effects of the environmental and
361 spatial or temperature related factors. This is because following the natural bending of the river,
362 rip-raps covered the right and left bank upstream and downstream of the outflow, respectively,
363 while natural stretches showed the reverse distribution. Nevertheless, the three-way interaction
364 in the data set among season, location and bank side, clearly shows that the structure of fish
365 assemblages can vary largely inshore, which indicates no clearly detectable role of thermal
366 pollution effects. Overall, this result corresponds with the results of Teixeira et al. (2012) who
367 found that structural diversity/complexity of the habitat was an important determinant of fish
368 assemblage structure in the vicinity of an NPP in the coastal area in Southern Brazil. In that
369 study, thermal pollution affected fish assemblages rather in an indirect manner, by decreasing
370 benthic cover of corals, macroalgae and sponges, which in turn decreased structural complexity
371 that exerted a strong effect on fish habitat use. However, fish assemblages remained unaffected
372 at sites with complex physical habitat structure. These results indicate the critical importance
373 of habitat structure in assessing and mitigating the effects of thermal pollution on the structure
374 of fish assemblages.

375 Contrary to inshore patterns, offshore fish assemblage structure was determined more by spatial
376 variability than merely hydrogeomorphological (i.e., environmental) effects. Nevertheless, the
377 overall explained variance was low, and, importantly, almost zero for the relative abundance
378 data. The seasonally and spatially variable abundance of species confirms our former findings
379 that fish show very elusive habitat responses to the relatively short environmental gradients
380 offshore (Szalóky et al., 2021).

381 A further step towards applying the results may be assessing the cumulative impact of not just
382 one, but more point source heat effluents. Our findings here (i.e., that the thermal effluent
383 entering from the right only affected the right shoreline zone) suggest that it is important to take

384 account on whether these point sources are located on the same or on different sides of the river.
385 Naturally, the effect of such point source thermal pollutions also depends largely on the
386 differences in discharge and temperature patterns between the effluents and the recipient river.
387 Although, series of thermal pollution effects are rare in single rivers, there are some notable
388 exceptions. For example, in Europe a large fraction of the flow of the Rhine, the Weser and the
389 Po Rivers are affected by thermal pollution (Raptis et al., 2016). It is thus important to study
390 the cumulative impact of thermal pollution effects in river systems, especially with the
391 acceleration of global warming.

392 In conclusion, although several studies have shown clear evidence of a variety of effects of
393 NPPs on biotic assemblages, we found that the Paks NPP exerts only a local scale effect on the
394 structure of Danubian fish assemblages. This might be due to the fact, that the outflow does not
395 significantly influence the hydrogeomorphical features and thermal conditions of the river,
396 relative to natural and other human induced variability, or at most only at a very small spatial
397 extent. In fact, we found that the spatiotemporal structure of fish assemblages can vary largely
398 both inshore and offshore, which dynamics overrule the effect of the artificially elevated
399 temperature. This study thus highlights the importance of the examination of
400 hydrogeomorphological variability of rivers and their effects on fish assemblage variability
401 when examining spatial effects of thermal pollution.

402

403 **Acknowledgements**

404 Prepared with the professional support of the Doctoral Student Scholarship Program of the Co-
405 operative Doctoral Program of the Ministry for Innovation and Technology from the source of
406 the National Research, Development and Innovation Fund. This study was supported by an
407 MTA KEP grant. The research presented in the article was carried out within the framework of
408 the Széchenyi Plan Plus program with the support of the RRF 2.3.1 21 2022 00008 project.

409

410 **Significance statement to the general public**

411 We examined the effect of a nuclear power plant's warmwater inflow on habitat and
412 temperature conditions and on the structure of fish assemblages in the Danube River, Hungary.
413 We found that the outflow exerted only a local scale effect on hydromorphology and fish
414 assemblage structure. The effect of the returned cooling water was more apparent in the
415 seasonally recorded surface water temperatures and depended highly on the spatial positioning
416 of the sampling sites. Our study highlights the importance of the assessment of
417 hydrogeomorphological variability of rivers and their influence on fish assemblage variability
418 when examining spatial effects of thermal pollution.

419

420 **Literature**

421 Adamantiades, A., & Kessides, I. (2009). Nuclear power for sustainable development: current
422 status and future prospects. *Energy Policy*, 37, 5149–5166.

423 <https://doi.org/10.1016/j.enpol.2009.07.052>

424 Baranya, S., & Józsa, J. (2007). Numerical and laboratory investigation of the hydrodynamic
425 complexity of a river confluence. *Periodica Polytechnica Civil Engineering*, 51, 3–8.
426 <https://doi.org/10.3311/pp.ci.2007-1.01>

427 Baranya, S., Olsen, N. R. B., & Józsa, J. (2015). Flow analysis of a river confluence with field
428 measurements and RANS model with nested grid approach. *River Research and Applications*,
429 31, 28–41. <https://doi.org/10.1002/rra.2718>

430 Benda, L., Andras, K., Miller, D., & Bigelow, P. (2004). Confluence effects in rivers:
431 Interactions of basin scale, network geometry, and disturbance regimes. *Water Resources*
432 *Research*, 40, W05402. <https://doi.org/10.1029/2003WR002583>

433 Boyer, C., Roy, A. G., & Best, J. L. (2006). Dynamics of a river channel confluence with
434 discordant beds: flow turbulence, bed load sediment transport, and bed morphology. *Journal of*
435 *Geophysical Research*, 111, F04007. <https://doi.org/10.1029/2005JF000458>

436 Bradbrook, K. F., Lane, S. N., Richards, K. S., & Biron, P. A. (2000). Large eddy simulation
437 of periodic flow characteristics at river channel confluences. *Journal of Hydraulic Research*,
438 38, 207–215. <https://doi.org/10.1080/00221680009498338>

439 Crawley, M. J. (2015). *Statistics: An Introduction Using R*. 2nd edition. John Wiley & Sons:
440 Chichester, UK. ISBN: 978-1-118-94109-6

441 Czeglédi, I., Sály, P., Takács, P., Dolezsai, A., Nagy, S. & Erős, T. (2015). The scales of
442 variability of stream fish assemblage at tributary confluences. *Aquatic Sciences*, 78,641–654.
443 <https://doi.org/10.1007/s00027-015-0454-z>

444 Daufresne, M., Roger, M. C., Capra, H., & Lamouroux, N. (2003). Long-term changes within
445 the invertebrate and fish communities of the Upper Rhône River: effects of climatic factors.
446 *Global Change Biology*, 10, 124–140. <https://doi.org/10.1046/j.1529-8817.2003.00720.x>

447 Descy, J. P., & Mouvet, C. (1984). Impact of the Tihange nuclear power plant on the periphyton
448 and the phytoplankton of the Meuse River (Belgium). *Hydrobiologia*, 119, 119–128.
449 <https://doi.org/10.1007/BF00011951>

450 Dudgeon, D., Arthington, A., Gessner, M., Kawabata, Z., Knowler, D., Lévêque, C., Naiman,
451 R. J., Prieur-Richard, A-H., Soto, D., Stiassny, M. L. J., & Sullivan, C. A. (2006). Freshwater
452 biodiversity: Importance, threats, status and conservation challenges. *Biological Reviews*, 81,
453 163–182. <https://doi.org/10.1017/S1464793105006950>

454 Erős, T., Tóth, B., Sevcsik, A., & Schmera, D. (2008). Comparison of Fish Assemblage
455 Diversity in Natural and Artificial Rip-Rap Habitats in the Littoral Zone of a Large River (River
456 Danube, Hungary). *International Review of Hydrobiology*, 93, 88–105.
457 <https://doi.org/10.1002/iroh.200710976>

458 Erős, T., Takács, P., Czeglédi, I., Sály, P., & Specziár, A. (2015). Taxonomic and trait based
459 recolonization dynamics of a riverine fish assemblage following a large scale human induced
460 disturbance: the red mud disaster in Hungary. *Hydrobiologia*, 758, 31–45.
461 <https://doi.org/10.1007/s10750-015-2262-9>

462 Erős, T. & Lowe, W. (2019). The Landscape Ecology of Rivers: from Patch-Based to Spatial
463 Network Analyses. *Current Landscape Ecology Reports*, 4, 103–112.
464 <https://doi.org/10.1007/s40823-019-00044-6>

465 Gutreuter, S., Vallazza, J. M., & Knights, B. C. (2009). Lateral distribution of fishes in the
466 main-channel trough of a large floodplain river: Implications for restoration. *River Research
467 and Applications*, 26, 619–635. <https://doi.org/10.1002/rra.1271>

468 Jan, R-Q., Chen, J-P., Lin, C-Y., & Shao, K-T. (2001). Long-term monitoring of the coral reef
469 fish communities around a nuclear power plant. *Aquatic Ecology*, 35, 233–243.
470 <https://doi.org/10.1023/A:1011496117632>

471 Janovics, R., Bihari, Á., Papp, L., Dezső, Z., Major, Z., Sárkány, K. E., Bujtás, T., Veres, M.,
472 & Palcsu, L. (2014). Monitoring of tritium, ⁶⁰Co and ¹³⁷Cs in the vicinity of the warm water
473 outlet of The Paks Nuclear Power Plant, Hungary. *Journal of Environmental Radioactivity*, 128,
474 20–26, <https://doi.org/10.1016/j.jenvrad.2013.10.023>

475 Jones, N. E., & Schmidt, B. J. (2016). Tributary effects in rivers: interactions of spatial scale,
476 network structure, and landscape characteristics. *Canadian Journal of Fisheries and Aquatic
477 Sciences*, 74, 503–510. <https://doi.org/10.1139/cjfas-2015-0493>

478 Karakosta, C., Pappas, C., Marinakis, V., & Psarras, J. (2013). Renewable energy and nuclear
479 power towards sustainable development: Characteristics and prospects. *Renewable and
480 Sustainable Energy Reviews*, 22, 187–197. <https://doi.org/10.1016/j.rser.2013.01.035>

481 Matthews W. J. (1998). *Patterns in Freshwater Fish Ecology*. Chapman & Hall: New York,
482 USA. <https://doi.org/10.1007/978-1-4615-4066-3>

483 Raptis, C. E., van Vliet, M. T. H., & Pfister, S. (2016). Global thermal pollution of rivers from
484 thermoelectric power plants. *Environmental Research Letters*, 11, 104011.
485 <https://doi.org/10.1088/1748-9326/11/10/104011>

486 Reid, A. J., Carlson, A. K., Creed, I. F., Eliason, E. J., Gell, P. A., Johnson, P. T. J., Kidd, K.
487 A., MacCormack, T. J., Olden, J. D., Ormerod, S. J., Smol, J. P., Taylor, W. W., Tockner, K.,
488 Vermaire, J. C., Dudgeon, D. & Cooke, S. J. (2019). Emerging threats and persistent
489 conservation challenges for freshwater biodiversity. *Biological Reviews*, 94, 849–873.
490 <https://doi.org/10.1111/brv.12480>

491 Rhoads, B. L., & Sukhodolov, A. N. (2001). Field investigation of three-dimensional flow
492 structure at stream confluences: 1. Thermal mixing and time-averaged velocities. *Water
493 Resources Research*, 37, 2393–2410. <https://doi.org/10.1029/2001WR000316>

494 Rice, S. P., Ferguson, R. I., & Hoey, T. B. (2006). Tributary control of physical heterogeneity
495 and biological diversity at river confluences. *Canadian Journal of Fisheries and Aquatic
496 Sciences*, 63, 2553–2566. <https://doi.org/10.1139/f06-145>

497 Schiel, D. R., Steinbeck, J. R., & Foster, M. S. (2004). Ten years of induced ocean warming
498 causes comprehensive changes in marine benthic communities. *Ecology*, 85, 1833–1839.
499 <https://doi.org/10.1890/03-3107>

500 Szalóky, Z., György, Á. I., Tóth, B., Sevcsik, A., Specziár, A., Csányi, B., Szekeres, J., & Erős,
501 T. (2014). Application of an electrified benthic frame trawl for sampling fish in a very large

502 European river (the Danube River) – Is offshore monitoring necessary? *Fisheries Research*,
503 151, 12–19. <https://doi.org/10.1016/j.fishres.2013.12.004>

504 Szalóky, Z, Füstös, V, Tóth, B, & Erős, T. (2021). Environmental drivers of benthic fish
505 assemblages and fish-habitat associations in offshore areas of a very large river. *River Research*
506 *and Applications*, 37, 712–721. <https://doi.org/10.1002/rra.3793>

507 Széchy, M. T. M, Koutsoukos, V. S., & Barboza, C. A. M. (2017). Long-term decline of brown
508 algal assemblages from southern Brazil under the influence of a nuclear power plant. *Ecological*
509 *Indicators*, 80, 258–267. <https://doi.org/10.1016/j.ecolind.2017.05.019>

510 Szupiany, R. N., Amsler, M. L., Parsons, D. R., & Best, J. L. (2009). Morphology, flow
511 structure, and suspended sediment transport at two large braid-bar confluences. *Water*
512 *Resources Research*, 45, W05415. <https://doi.org/10.1029/2008WR007428>

513 Teixeira, T. P., Neves, L. M, & Araújo, F. G. (2009). Effects of a nuclear power plant thermal
514 discharge on habitat complexity and fish community structure in Ilha Grande Bay, Brazil.
515 *Marine Environmental Research*, 68, 188–195.
516 <https://doi.org/10.1016/j.marenvres.2009.06.004>

517 Teixeira, T. P., Neves, L. M, & Araújo, F. G. (2012). Thermal impact of a nuclear power plant
518 in a coastal area in Southeastern Brazil: effects of heating and physical structure on benthic
519 cover and fish communities. *Hydrobiologia*, 684, 161–175. <https://doi.org/10.1007/s10750-011-0980-1>

521 Wolter, C., & Bischoff, A. (2001). Seasonal changes of fish diversity in the main channel of
522 the large lowland river Oder. *Regulated Rivers: Research & Management*, 17, 595–608.
523 <https://doi.org/10.1002/rrr.645>

524 Wolter, C., & Freyhof, J. (2004). Diel distribution patterns of fishes in a temperate large
525 lowland river. *Journal of Fish Biology*, 64, 632–642. <https://doi.org/10.1111/j.1095-8649.2004.00327.x>

526

527 **Figure captions**

528

529 **Fig. 1.** Map of the study area and location of the sampling units upstream and downstream
530 from the warm water effluent (indicated by red arrow) of the Paks nuclear power plant in the
531 Danube River, Hungary. R and N letters indicate the location of rip-rap (R) and natural (N)
532 shoreline sampling units, while light blue blocks with numbers show the location of surveyed
533 subreaches. The flow direction is shown by a blue arrow on top. Two groins are indicated by
534 two black polygons in subreach No. 1 and 4 (yellow arrows pointing towards).

535

536 **Fig. 2.** Depth maps of the subreaches a) in spring, b) in summer and c) in autumn. Flow
537 direction and the warm effluent are indicated by a blue and a red arrow, respectively. Seasonal
538 differences are closely following the differences in measured flow discharges (1700, 2700 and
539 $1800 \text{ m}^3\text{s}^{-1}$, respectively). The local scouring effect of the two groins in subreach No. 1 and 4
540 is clearly visible. Otherwise the bathymetry of the study area is characterized by the two
541 subsequent bends, with no apparent anthropogenic influence.

542

543 **Fig. 3.** Velocity maps of the subreaches a) in spring, b) in summer and c) in autumn. Flow
544 direction and the warm effluent are indicated by a blue and a red arrow, respectively. The
545 coherence here with seasonal discharges is weaker than by the depth maps. The shading effect
546 of the groins can be seen as lower velocity values near them. The narrowing of the streamline
547 in subreach No. 4 may be the only and also low influence of the warm effluent.

548

549 **Fig. 4.** Substrate composition of the study area determined on subreach-level. Flow direction
550 and the warm effluent are indicated by a blue and a red arrow, respectively. The studied reach
551 is dominated by sand and gravel, while silt and cobble are uniformly minimal or missing,
552 respectively. No apparent influence of the effluent was observed.

553

554 **Fig. 5.** Temperature maps of the subreaches a) in spring, b) in summer and c) in autumn. Flow
555 direction and the warm effluent are indicated by a blue and a red arrow, respectively. A clear
556 heat tail, separated from the ambient temperature is visible in all three subfigures. Note that
557 the left bank is unaffected on the entire reach. A side arm on the right bank diverts the warm
558 flow, which then returns between subreaches No. 5 and 6, hence the higher temperatures in
559 subreach No. 6.

560

561

Fig. 1.

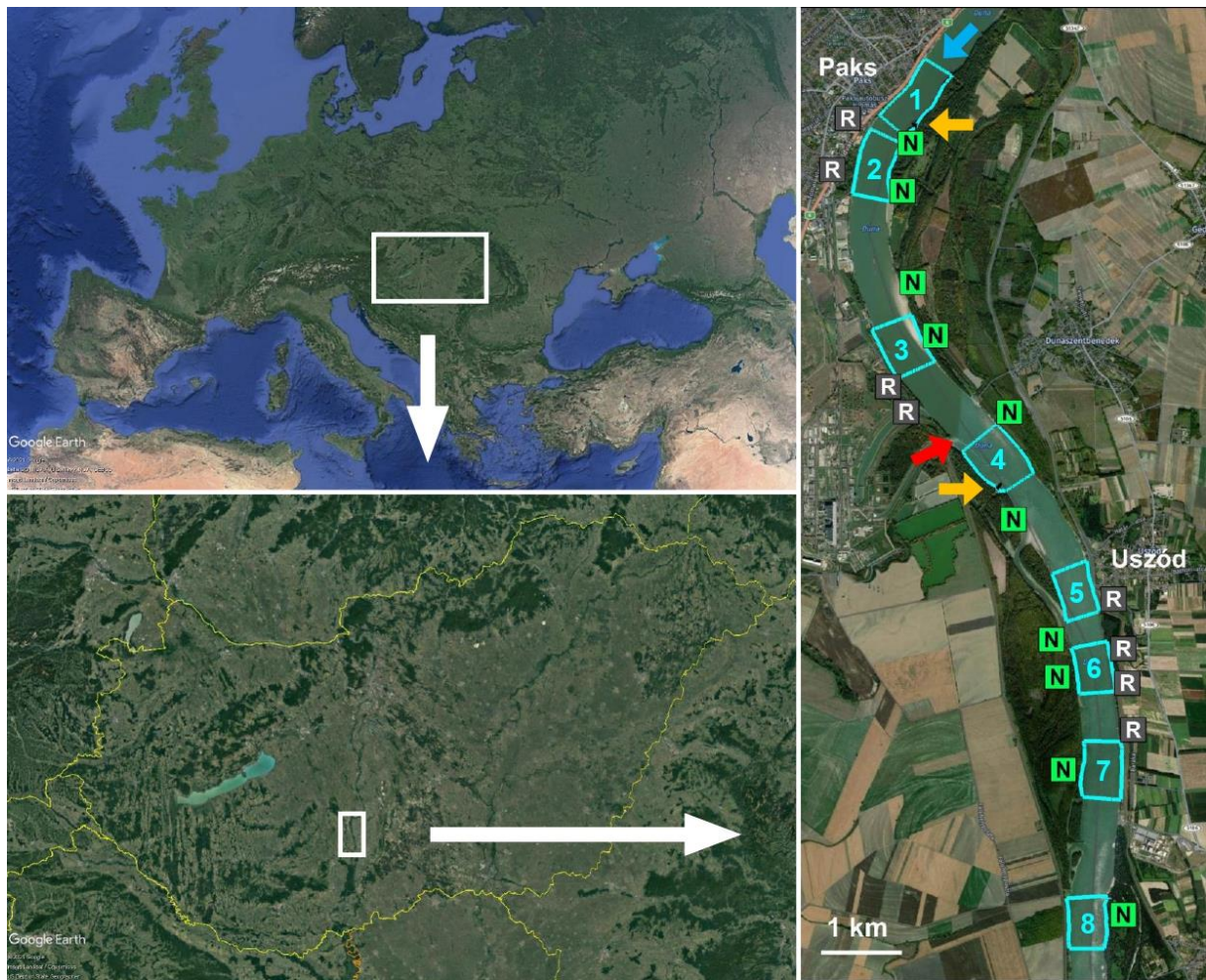




Fig. 3.



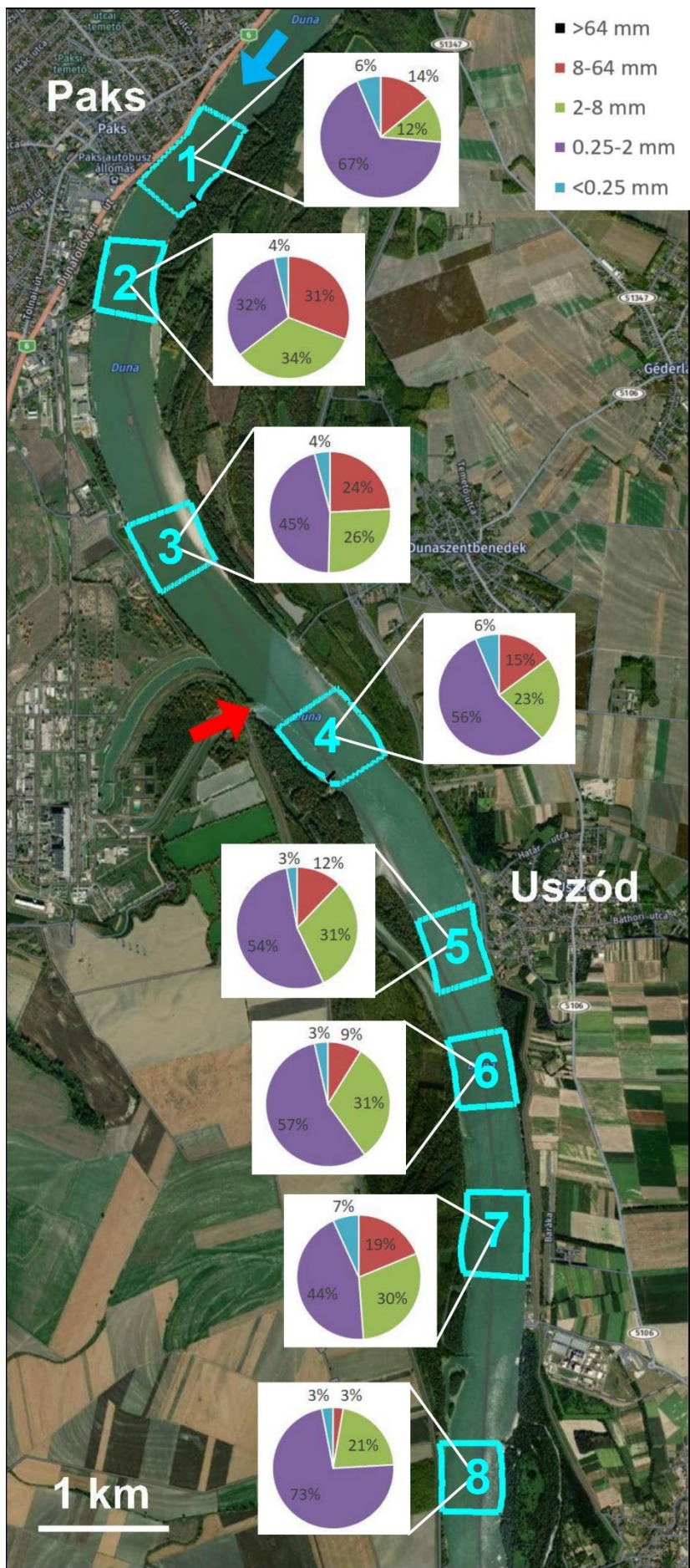
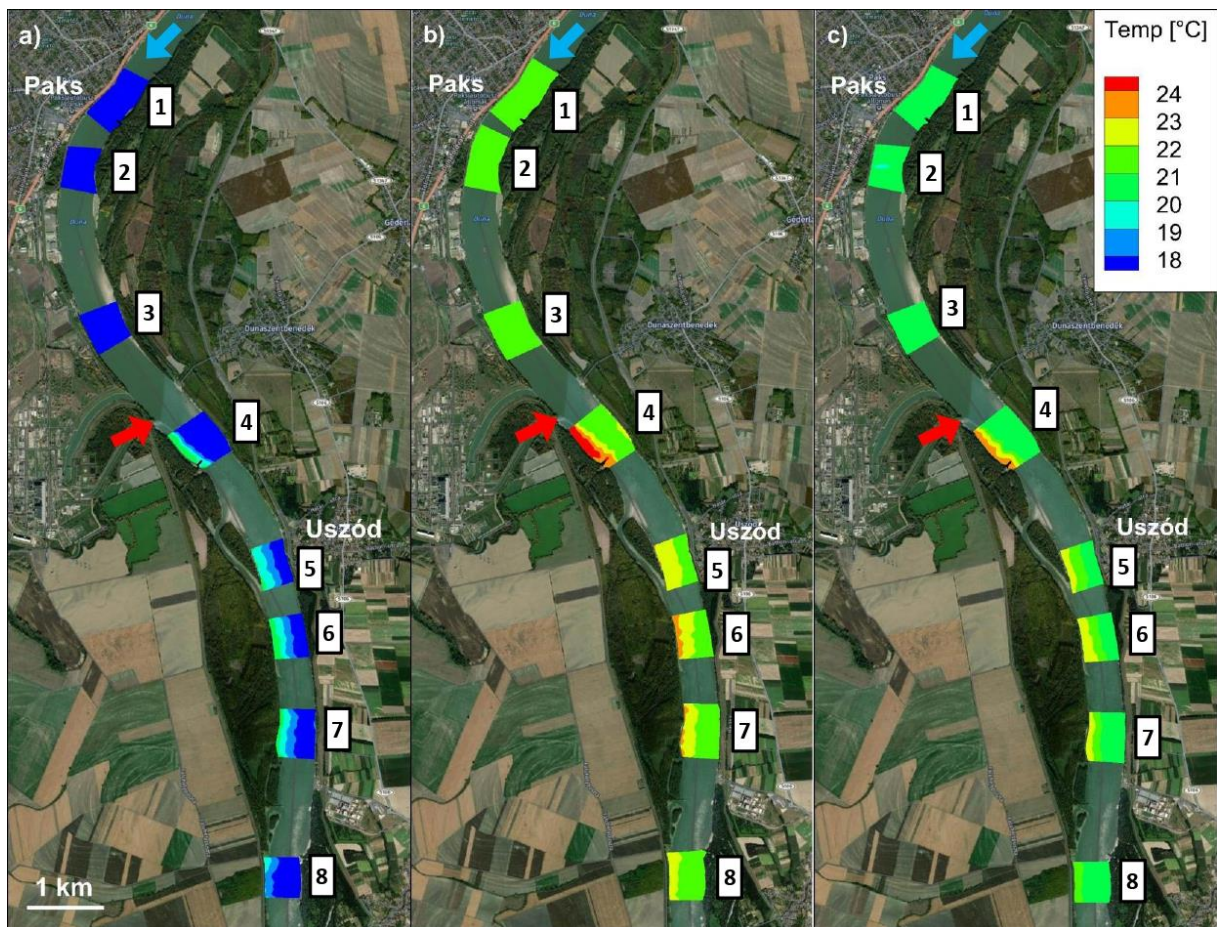


Fig. 4.



567 **Tables**

568

569 **Table 1.** Anova table of the minimal adequate GLM model used to explore the relationships
570 between shoreline water temperature (response variable) and spatial location of the sampling
571 sites and seasons (explanatory factors). Bank, two-leveled factor coding the right and left side
572 of the river. Location, two-leveled factor coding the upstream or downstream location of the
573 sampling sites to the outflow of the power plant. Season, a three leveled factor coding the
574 spring, summer, and autumn sampling sessions. Colons denote interaction between the
575 factors.

	Df	Sum of Sq	F statistics	p-value
bank	1	7.7	252.3	< 0.001
location	1	28.5	931.2	< 0.001
season	2	161.9	2641.5	< 0.001
bank:location	1	14.2	463.8	< 0.001
bank:season	2	0.8	13.1	< 0.001
location:season	2	3.0	48.5	< 0.001
bank:location:season	2	0.9	14.9	< 0.001

576

577 **Table 2.** Anova table of the minimal adequate GLM model used to explore the relationships
 578 between offshore water temperature (response variable) and spatial location of the sampling
 579 sites and seasons (explanatory factors). Position, five-leveled factor coding the location along
 580 the cross-section of the river. Location, two-leveled factor coding the upstream or
 581 downstream location of the sampling sites to the outflow of the power plant. Season, a three
 582 leveled factor coding the spring, summer, and autumn sampling sessions. Colons denote
 583 interaction between the factors.

	Df	Sum of Sq	F statistics	p-value
position	4	8	15.06	< 0.001
location	1	25	184.83	< 0.001
season	2	399	1491.38	< 0.001
position:location	4	5	9.82	< 0.001
location:season	2	2	5.69	0.005

584

Table 3. The fish species collected in the Danube River and their relative abundance in the inshore and offshore samples.

Species name	Common name	Code	Total	Offshore samples			Inshore samples				
				Sum	Spring	Summer	Autumn	Sum	Spring	Summer	Autumn
<i>Alburnus alburnus</i> (Linnaeus, 1758)	Bleak	albalb	42.05	1.14	1.52	0.61	1.47	49.53	32.35	57.82	54.77
<i>Romanogobio vladykovi</i> (Fang, 1943)	White-finned gudgeon	romvla	14.54	41.47	36.87	51.27	34.72	9.61	3.10	12.27	11.82
<i>Neogobius melanostomus</i> (Pallas, 1814)	Round goby	neomel	14.24	29.64	22.98	23.40	37.22	11.42	25.37	2.72	8.09
<i>Blicca bjoerkna</i> (Linnaeus 1758)	White bream	blibjo	7.74	2.48	2.78	1.93	2.85	8.71	10.63	7.76	8.13
<i>Leuciscus idus</i> (Linnaeus, 1758)	Ide	leuidu	3.88	0.39	0.25	0.10	0.69	4.52	9.24	3.43	2.52
<i>Chondrostoma nasus</i> (Linnaeus, 1758)	Common nase	chonas	2.89	1.30	1.77	1.83	0.69	3.18	5.38	4.48	1.41
<i>Sander lucioperca</i> (Linnaeus, 1758)	Pike-perch	sanluc	2.09	0.47	0.25	0.61	0.43	2.38	2.75	2.19	2.27
<i>Zingel streber</i> (Siebold, 1863)	Danube streber	zinstr	2.04	13.17	13.38	16.28	10.45	0.00	0.00	0.00	0.00
<i>Ponticola kessleri</i> (Günter, 1861)	Bighead goby	ponkes	1.27	0.32	0.00	0.10	0.60	1.44	1.39	0.80	1.77
<i>Rutilus pigus</i> (Lacepède, 1803)	Danube Roach	rutpig	1.24	0.51	1.26	0.00	0.69	1.38	0.71	0.62	2.09
<i>Ballerus sapa</i> (Pallas, 1814)	White-eye bream	balsap	1.10	1.18	1.26	0.61	1.64	1.08	2.04	0.99	0.62
<i>Gymnocephalus schraetser</i> (Linnaeus, 1758)	Schraetzer	gymsch	1.10	2.21	9.60	0.20	1.38	0.89	0.73	1.02	0.92
<i>Abramis brama</i> (Linnaeus, 1758)	Freshwater bream	abrbra	1.08	1.77	2.27	0.81	2.42	0.95	1.28	2.32	0.14
<i>Leuciscus aspius</i> (Linnaeus, 1758)	Asp	leuasp	0.68	0.04	0.00	0.00	0.09	0.79	0.73	1.05	0.71
<i>Babka gymnotrachelus</i> (Kessler, 1857)	Racer goby	babgym	0.67	0.35	0.00	0.20	0.60	0.73	0.16	0.37	1.19
<i>Vimba vimba</i> (Linnaeus, 1758)	Vimba bream	vimvim	0.46	0.55	2.53	0.20	0.17	0.45	1.28	0.09	0.17
<i>Zingel zingel</i> (Linnaeus, 1766)	Zingel	zinzin	0.41	0.59	1.01	0.41	0.60	0.38	0.11	0.06	0.68
<i>Squalius cephalus</i> (Linnaeus, 1758)	Chub	squcep	0.41	0.00	0.00	0.00	0.00	0.48	0.35	0.49	0.55
<i>Sander volgensis</i> (Gmelin, 1789)	Volga pikeperch	sanvol	0.35	0.08	0.00	0.00	0.17	0.40	0.08	0.15	0.69
<i>Barbus barbus</i> (Linnaeus, 1758)	Barbel	barbar	0.35	1.46	2.27	0.61	1.90	0.15	0.14	0.12	0.17
<i>Silurus glanis</i> (Linnaeus, 1758)	Wels catfish	silgla	0.31	0.39	0.00	0.41	0.52	0.30	0.41	0.37	0.20
<i>Lota lota</i> (Linnaeus, 1758)	Burbot	lotlot	0.30	0.00	0.00	0.00	0.00	0.36	0.76	0.00	0.32
<i>Rutilus rutilus</i> (Linnaeus, 1758)	Roach	rutrut	0.19	0.04	0.00	0.00	0.09	0.22	0.24	0.46	0.09
<i>Neogobius fluviatilis</i> (Pallas, 1814)	Monkey goby	neoflu	0.13	0.00	0.00	0.00	0.00	0.16	0.05	0.09	0.24
<i>Perca fluviatilis</i> (Linnaeus, 1758)	European perch	perflu	0.12	0.00	0.00	0.00	0.00	0.14	0.05	0.12	0.19

<i>Proterorhinus semilunaris</i> (Heckel, 1837)	Western tubenose goby	prosem	0.08	0.12	0.00	0.10	0.17	0.07	0.03	0.00	0.13
<i>Carassius gibelio</i> (Bloch, 1782)	Prussian carp	cargib	0.07	0.04	0.00	0.10	0.00	0.08	0.30	0.00	0.00
<i>Cyprinus carpio</i> (Linnaeus, 1758)	Common carp	cypcar	0.05	0.04	0.00	0.10	0.00	0.05	0.11	0.06	0.01
<i>Esox lucius</i> (Linnaeus, 1758)	Northern pike	esoluc	0.04	0.00	0.00	0.00	0.00	0.05	0.08	0.00	0.06
<i>Gymnocephalus baloni</i> (Holčík & Hensel, 1974)	Danube ruffe	gymbal	0.03	0.00	0.00	0.00	0.00	0.04	0.08	0.00	0.03
<i>Gymnocephalus cernua</i> (Linnaeus, 1758)	Ruffe	gymcer	0.02	0.00	0.00	0.00	0.00	0.02	0.05	0.03	0.00
<i>Hypophthalmichthys molitrix</i> (Valenciennes, 1844)	Silver carp	hypmol	0.02	0.00	0.00	0.00	0.00	0.02	0.00	0.09	0.00
<i>Acipenser ruthenus</i> (Linnaeus, 1758)	Sterlet sturgeon	acirut	0.02	0.12	0.00	0.10	0.17	0.00	0.00	0.00	0.00
<i>Pelecus cultratus</i> (Linnaeus, 1758)	Sichel	pelcul	0.01	0.08	0.00	0.00	0.17	0.00	0.00	0.00	0.00
<i>Eudontomyzon mariae</i> (Berg, 1931)	Ukrainian brook lamprey	eudmar	0.01	0.00	0.00	0.00	0.00	0.01	0.00	0.00	0.01
<i>Ballerus ballerus</i> (Linnaeus, 1758)	Zope	balbal	0.01	0.04	0.00	0.00	0.09	0.00	0.00	0.00	0.00
Number of specimens collected			16398	2537	396	983	1158	13861	3678	3236	6947

588 **Table 4.** Permutation test (n=2000) by terms under the reduced model of the partial
 589 redundancy analysis modelling logarithm transformed ($x' = \ln(x+1)$) species richness of the
 590 shoreline samples (response). Colons indicate interaction between the factors.

	Df	Variance	F statistics	p-value
season	2	0.00811	6.275	0.004
location	1	0.00027	0.417	0.524
bank	1	0.00002	0.032	0.870
season:location	2	0.00220	1.702	0.209
season:bank	2	0.00138	1.068	0.348
location:bank	1	0.00122	1.886	0.175
season:location:bank	2	0.00603	4.669	0.016

591

592 **Table 5.** Permutation test (n=2000) by terms under the reduced model of the partial
593 redundancy analysis modelling the logarithm transformed ($x' = \ln(x+1)$) species richness of
594 the offshore samples (response). Colons indicate interaction between the factors.

	Df	Variance	F statistics	p-value
season	2	0.03622	14.255	< 0.001
location	1	0.00201	1.583	0.214
position	4	0.00854	1.681	0.173
season:location	2	0.00766	3.016	0.054
season:position	8	0.01766	1.737	0.104
location:position	4	0.00461	0.907	0.464
season:location:position	8	0.02006	1.974	0.063

595

596 **Table 6.** Permutation test (n=2000) by terms under the reduced model of the partial
 597 redundancy analysis modelling the Hellinger transformed composition of fish abundances in
 598 the shoreline samples. Colons indicate interaction between the factors.

	Df	Variance	F statistics	p-value
season	2	0.02947	5.543	< 0.001
location	1	0.00635	2.389	0.021
bank	1	0.00282	1.062	0.367
season:location	2	0.00407	0.765	0.718
season:bank	2	0.01119	2.104	0.012
location:bank	1	0.00413	1.555	0.136
season:location:bank	2	0.01384	2.603	0.002

599

600 **Table 7** Permutation test (n=2000) by terms under the reduced model of the partial
 601 redundancy analysis modelling the Hellinger transformed composition of fish abundances in
 602 the offshore samples. Colons indicate interaction between the factors.
 603

	Df	Variance	F statistics	p-value
season	2	0.01648	3.297	< 0.001
location	1	0.00395	1.580	0.108
position	4	0.02720	2.720	<0.001
season:location	2	0.00940	1.879	0.015
season:position	8	0.01796	0.898	0.729
location:position	4	0.01172	1.172	0.214
season:location:position	8	0.01635	0.818	0.861

604